Suppression of elastic scattering loss for slowly colliding Bose-Einstein condensates

Y. B. Band,[1,2] J. P. Burke, Jr.,[2] A. Simoni,[2,3] and P. S. Julienne[2]
[1]*Department of Chemistry, Ben-Gurion University of the Negev, Beer-Sheva 84105, Israel*
[2]*Atomic Physics Division, A267 Physics, National Institute of Standards and Technology, Gaithersburg, Maryland 20899*
[3]*INFM–European Laboratory (LENS) and Università di Firenze, Largo E. Fermi 2, I-50125 Firenze, Italy*
(Received 2 March 2001; published 13 July 2001)

Superfluid suppression of the elastic scattering loss in atomic Bose condensed systems can be significant when the ratio of the relative velocity of the wave packets to the critical velocity is ~ 1. We show how to incorporate the effect of such losses and their suppression into the time-dependent dynamics of two colliding condensate wave packets. We illustrate the magnitude of the effect through three-dimensional simulations of the collision dynamics of an $|F=2, M_F=2\rangle$ with an $|F=2, M_F=1\rangle$ ^{87}Rb condensate in a harmonic trap, as studied in a recent experiment [Maddaloni *et al.*, Phys. Rev. Lett. **85**, 2413 (2000)]. These calculations show that the effect of elastic scattering and its suppression should be seen in the oscillatory center-of-mass amplitude of the $M_F=1$ wave packet for suitable experimental conditions.

DOI: 10.1103/PhysRevA.64.023607 PACS number(s): 03.75.Fi, 67.90.+z, 71.35.Lk

I. INTRODUCTION

In a recent paper [1], we pointed out the importance of elastic scattering loss (ESL) in Bose-Einstein condensate (BEC) collision dynamics involving wave packets having disparate velocity components. When one BEC wave packet with velocity $\mathbf{v}_1$ moves through another BEC wave packet with velocity $\mathbf{v}_2$, the collision of an atom from wave packet 1 with one from wave packet 2 results in elastic scattering into all directions, and consequent loss of the atoms from the wave packets. Reference [1] only considered the high-velocity case, for which the relative speed v is large compared to the speed of sound v_s in the condensate so that the free-particle dispersion relation applies. Here, we consider the superfluid suppression of elastic scattering loss when v becomes comparable to v_s and the free-particle dispersion relation no longer applies. In particular, we give an example of a specific type of experiment involving the collision of two condensate wave packets that might yield information about superfluid suppression of ESL.

Quasiparticles are created in a zero-temperature condensate when an atom that is not part of the condensate is scattered off the condensate. A suppression of scattering occurs due to the superfluidity of the condensate whenever the atom has a velocity relative to the center of mass (c.m.) of the condensate that is either slower than or comparable to v_s [2,3]. A recent experiment [4] demonstrated such suppression of ESL when an impurity atom with a velocity on the order of v_s moves through a Na BEC. Recent theoretical studies have also examined the effect of trap shape on such suppression [5] and the effect of suppression on sympathetic cooling [6].

Moving BEC wave packets can be created by a variety of means, such as Bragg [7] or Raman [8] outcoupling. In a recent experiment by Maddaloni *et al.* [9], a radio frequency (rf) pulse was used to convert a fraction of condensed ^{87}Rb atoms from the $|F=2, M_F=2\rangle$ to the $|2,1\rangle$ hyperfine state. The $|2,1\rangle$ BEC wave packet then undergoes oscillatory motion in its harmonic potential, which has a smaller frequency than the $|2,2\rangle$ potential and is displaced by gravity from that of the $|2,2\rangle$ potential (see Fig. 1). The displacement of the $|2,1\rangle$ trap is much larger than the size of the condensates. Therefore, the two wave packets overlap and collide near the end of each oscillation cycle as the relative velocity decreases from a finite value to zero. Suppression of ESL should be important in this regime. Although we show that information about the suppression of ESL is difficult to extract from this specific experiment, we find that similar experiments with larger numbers of condensed atoms could yield detailed information about superfluid suppression of ESL. It may be easier to experimentally characterize the oscillatory motion of the BEC wave packets than to count atom loss as in Ref. [4]. Furthermore, suppression of ESL, and its effect on BEC dynamics, may play important roles in other experiments such as the bouncing of BECs off a mirror or beam splitter formed by a far-detuned light sheet [10] and other types of devices that manipulate BEC wave packets. Here we develop a theory capable of modeling such experiments and we explicitly compare with the experimental results of Ref. [9]. Section II describes the specific physical system we study, and the incorporation of ESL and its suppression into the time-dependent Gross-Pitaevskii equation for moving BEC wave packets. Section III presents our calculated results and a final section summarizes our conclusions.

II. THEORY

A. Physical system

The physical system that we have is two colliding BEC wave packets in different spin states. Although there are a number of experimental scenarios for such collisions, for the sake of concrete illustration we will keep in mind the geometry of the recent experiment by Maddaloni *et al.* [9] that we described in the Introduction. Due to the different magnetic moments of the $|2,2\rangle$ and $|2,1\rangle$ states, and the effect of gravity, these states are trapped in different potentials whose minima are displaced along the direction of gravity (labeled as the *y* axis in Fig. 1) by a distance larger than the initial size of each condensate wave packet. As a consequence, the $|2,1\rangle$ cigar-shaped condensate (the axis of the cigar is oriented horizontally and is called the *z* axis), initially created

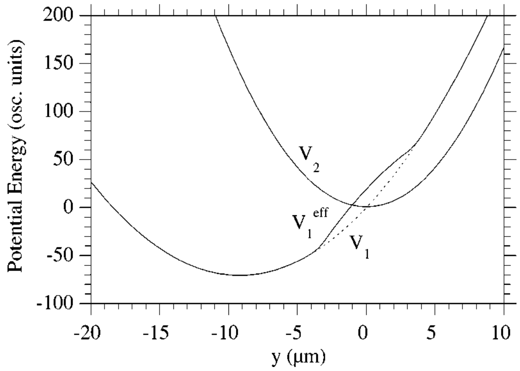

FIG. 1. Harmonic trapping potentials for the two spin components, $|2,2\rangle$ and $|2,1\rangle$. The solid line V_1^{eff} includes the mean-field overlap potential. The y axis is in the vertical direction.

identical in shape and size to the parent $|2,2\rangle$ condensate and at the equilibrium position of the parent condensate, undergoes large c.m. oscillations along the y axis. The two condensate wave packets interact as the $|2,1\rangle$ wave packet collides at the top of its oscillatory trajectory with the $|2,2\rangle$ wave packet. Our simulations show that (a) it is necessary to include ESL of atoms into the dynamics of the above-the-mean-field components, and (b) it can be important to include superfluid suppression of the ESL in the modeling of these experiments since the ratio of the relative velocity of the wave packets to v_s is not large.

In Ref. [9], $N=1.5\times10^5$ condensate atoms in state $|2,2\rangle$ are trapped in an asymmetric harmonic trap with angular frequencies $\omega_{z2}=2\pi\times12.6(2)$ Hz, and $\omega_{\perp 2}\equiv\omega_{x2}=\omega_{y2}=2\pi\times164.5(5)$ Hz, respectively. A $|2,1\rangle$ wave packet with $N_1\approx13\%\times N$ atoms is created by applying a short rf pulse, leaving $N_2\approx87\%\times N$ in the $|2,2\rangle$ state. To a very good approximation, the rf pulse makes a $|2,1\rangle$ copy of the parent $|2,2\rangle$ wave packet. The $|2,1\rangle$ trapping frequencies are $\omega_{j1}=\omega_{j2}/\sqrt{2}$, $j=1,2,3$, due to its smaller magnetic moment. In order to make a measurement of condensate dynamics, the trapping magnetic field is turned off after a variable time t_f from the onset of the rf pulse, after which the $|2,1\rangle$ and $|2,2\rangle$ wave packets expand and fall in gravity. The wave packets are imaged by absorption after being allowed to fall and expand for 30 ms. Section III describes the interpretation of these images in terms of condensate wave-packet collisions.

B. Theory of suppressed ESL losses

Using an analysis based upon Ref. [1], we model the dynamics of two colliding BEC wave packets using a generalization of the Gross-Pitaevskii equation (GPE) that accounts for elastic scattering loss (although the elastically scattered atoms cannot be described as part of the mean field):

$$\left[\frac{\partial}{\partial t}+\frac{i}{\hbar}\left(-\frac{\hbar^2}{2m}\boldsymbol{\nabla}^2+V_1(\mathbf{r},t)\right)\right]\psi_1 = -i\frac{4\pi\hbar}{m}(N_1a_{11}|\psi_1|^2+N_2a_{12}|\psi_2|^2)\psi_1 - \frac{v_r(t)\sigma(v_r)}{2}N_2|\psi_2|^2\psi_1, \tag{1}$$

$$\left[\frac{\partial}{\partial t}+\frac{i}{\hbar}\left(\frac{-\hbar^2}{2m}\boldsymbol{\nabla}^2+V_2(\mathbf{r},t)\right)\right]\psi_2 = -i\frac{4\pi\hbar}{m}(N_2a_{22}|\psi_2|^2+N_1a_{12}|\psi_1|^2)\psi_2 - \frac{v_r(t)\sigma(v_r)}{2}N_1|\psi_1|^2\psi_2. \tag{2}$$

The last terms on the right-hand side of Eqs. (1) and (2) model the ESL of atoms from the condensate wave packets. Here, $v_r(t)$ is the time-dependent relative velocity of the $|2,1\rangle$ and $|2,2\rangle$ components, and $\sigma(v_r)$ is the velocity-dependent elastic scattering cross section (see below). We make the approximation that we can ignore the spread in v_r across the wave packet and use the center-of-mass velocity of each packet to obtain a single v_r at each time t.

The energy dispersion relation for the quasiparticles created in a homogeneous $|2,2\rangle$ condensate upon scattering a probe atom is $\omega_q=v_sq\sqrt{1+(q/k_{\mathrm{coh}})^2}$, where q is the magnitude of the momentum transfer of the probe particle to the condensate, $k_{\mathrm{coh}}=\sqrt{16\pi n_2a_{22}}$ is the inverse coherence length, and $v_s=\sqrt{\hbar k_{\mathrm{coh}}/2m}=\sqrt{\mu/m}$ is the sound velocity. In the long wavelength limit, the dispersion relation is phonon-like, and incoherent scattering of atoms moving with velocities smaller than the speed of sound does not occur because energy and momentum cannot be simultaneously conserved if $v_r<v_c$. Here v_c is the critical velocity estimated by the Landau criterion to be equal to v_s, but recently assessed to be significantly smaller than v_s for inhomogeneous condensates [5]; for example, Ref. [5] found that $v_c\approx0.42v_s$ for the lowest mode of a particular condensate with cylindrical geometry. Moreover, for $v_r\gtrsim v_c$, a substantial suppression of elastic scattering occurs [4,6,11,12]. Superfluid suppression results in a velocity-dependent cross section, $\sigma(v_r)$. For $v_r/v_c\gg1$, the elastic scattering collision cross section reaches its nominal Wigner threshold value, $\sigma=4\pi a_{12}^2$, but otherwise the cross section is reduced to $\sigma(v_r)\equiv\Gamma/(n_1v_r)$:

$$\Gamma\equiv\frac{2\pi}{\hbar}\sum_{f,f'}\int d^3q\left|\frac{-4\pi\hbar^2T(q)}{mq}\langle\Psi_{1,f'}\Psi_{2,f}|\rho_{1,-\mathbf{q}}\rho_{2,\mathbf{q}}|\Psi_{1,i'}\Psi_{2,i}\rangle\right|^2\delta(E_f-E_i)$$
$$\approx\frac{2\pi}{\hbar}n_1\sum_f\int d^3q\left|\frac{4\pi\hbar^2a_{12}}{m}\langle\mathbf{q}+\mathbf{k}_i,\psi_{2,f}|\rho_{2,\mathbf{q}}|\mathbf{k}_i,\psi_2\rangle\right|^2\delta\left(\frac{[\hbar(\mathbf{q}+\mathbf{k}_i)]^2}{2m}+E_{2,f}-\frac{(\hbar\mathbf{k}_i)^2}{2m}-E_{2,i}\right)$$
$$=n_1v_r4\pi a_{12}^2\theta(v_r/v_c-1)[1-(v_r/v_c)^{-4}-4\ln(v_r/v_c)/(v_r/v_c)^2], \tag{3}$$

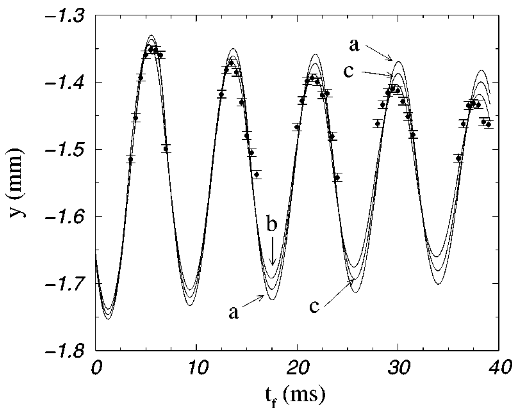

FIG. 2. Position of the center of mass of the $|2,1\rangle$ wave packet versus t_f after 30 ms of ballistic expansion. Experimental points taken from Ref. [1]. The theoretical curves calculated are (a) without elastic scattering loss, (b) with ESL using $\sigma = 4\pi a_{12}^2$, (c) with ESL using the suppressed elastic scattering cross section with $v_c = v_s$, and (d) with ESL using the suppressed elastic scattering cross section with $v_c = 0.42 v_s$. The latter, (d), is virtually indistinguishable from the results with unsuppressed elastic scattering, (b), and hence has not been included in the figure.

where the fundamental many-body form for the interaction between atoms involving the T matrix has been used [1,13,14], $\rho_{\mathbf{q}}$ is the Fourier transform of the particle density, and θ is the theta step function [hence when $v_r/v_c \leqslant 1$, $\sigma(v_r)=0$]. In this analysis, the scattering rate Γ [15] has been simplified to be appropriate for the case when the number of atoms in the $|2,1\rangle$ condensate is small so that its critical velocity is negligibly small and superfluid suppression of elastic scattering [4,6] for the $|2,1\rangle$ need not be considered. The generalization, treating $|2,1\rangle$ as a condensate that collides with the $|2,2\rangle$ condensate rather than as individual impurity atoms that collide with the $|2,2\rangle$, will be considered elsewhere. In our modeling, we calculate the relative collision velocity, $v_r(t)$, as follows: $v_r(t) = [|\langle\psi_1(t)|p_y|\psi_1(t)\rangle - \langle\psi_2(t)|p_y|\psi_2(t)\rangle|]/m$. Thus, we have for simplicity assumed that the internal velocities of the atoms in the condensate are small in comparison with $v_r(t)$, and therefore can be neglected in the determination of the relative velocity of the collisions.

III. RESULTS

A. Experiment and theory compared

We solve Eqs. (1) and (2) using standard fast Fourier transform techniques for time-dependent propagation. Our method uses a fully three-dimensional grid. We find that a grid with 32, 512, and 32 points in the *x*, *y*, and *z* directions is adequate for accurate calculations. In fact, our results without ESL are not significantly different from the simpler two-dimensional model used in Ref. [9].

Figure 2 compares our calculated $|2,1\rangle$ condensate c.m. position with the experimental data of Ref. [9] as a function of t_f, the time from the rf pulse to the time the trap is turned off. The measurement takes place 30 ms after the trap is turned off. The c.m. of the ith wave packet evolves during the free-fall evolution as

$$y_i(t) = y_i(t_f) + v_{y,i}(t_f)(t-t_f) + (g/2)(t-t_f)^2, \qquad (4)$$

where $t-t_f$ is the time when the trap is turned off, since the mean-field interaction between the condensates during free expansion is negligible [16]. When $v_{y,i}(t_f)$ is not close to zero, the second term in this equation is much larger at $t-t_f=30$ ms than the first term, $y_i(t_f)$ (the third term is a constant for $t-t_f=30$ ms). Hence, Fig. 2, which plots $y_i(t_f+30$ ms) versus t_f, approximately corresponds to plotting $v_{y,i}(t_f)$ versus t_f. The peak of the $|2,1\rangle$ c.m. trajectory corresponds to the largest upward moving $v_{y,i}(t_f)$, whereas the minimum of the trajectory corresponds to the largest downward moving (i.e., negative) $v_{y,i}(t_f)$. Figure 2 shows calculated results (a) without ESL, (b) with ESL using $\sigma = 4\pi a_{12}^2$, and (c) with ESL using the suppressed elastic scattering cross section, Eq. (3), with $v_c = v_s$. The figure does not show the case (d) with ESL where we take a suppressed elastic scattering cross section with $v_c = 0.42 v_s$, because this case is virtually indistinguishable from case (b) with unsuppressed elastic scattering.

The c.m. of the $|2,1\rangle$ wave packet exhibits a modified oscillation frequency that is significantly upshifted relative to $\omega_{\perp 1} = 2\pi \times 116.3$ Hz. The frequency shift is due to the interaction of the $|2,1\rangle$ with the $|2,2\rangle$ wave packet, which contributes to the effective interaction potential experienced by the $|2,1\rangle$ component: $V_1^{\mathrm{eff}} = V_1 + N_2(2\pi\hbar^2 a_{12}/m)|\psi_2|^2$ (see Fig. 1); the mean-field repulsion shifts the oscillation frequency. The measured frequency of the $|2,1\rangle$ c.m. motion is shifted to about 123.9 Hz, and our calculations yielded 122.7 Hz for case (b) with ESL and 122.5 Hz for case (a) without ESL. Thus, ESL does not have a significant effect on the frequency shift. However, Fig. 2 shows a clear loss of amplitude of the $|2,1\rangle$ c.m. motion that is due to two factors. Some of the kinetic energy of the $|2,1\rangle$ c.m. motion is converted into other degrees of freedom (mostly into the $|2,2\rangle$ c.m. kinetic energy). However, energy transfer cannot completely describe the amplitude loss seen in Ref. [9]. ESL affects the $|2,1\rangle$ c.m. motion because particles with high kinetic and potential energy are preferentially removed from the $|2,1\rangle$ wave packet, thereby resulting in lower c.m. energy after reequilibration. Comparison of the calculated curves in Fig. 2 with the experimental data shows that cases (b) and (d) compare well with the experimental amplitude [17]. Thus, ESL is important for this particular experimental case, but there is little evidence of suppression of ESL.

Figure 3 illustrates more fully the nature of the condensate collision dynamics and the effect of elastic scattering. The figure shows the following energies per particle versus t_f: the energies of each of component, $E_{|2,2\rangle}$ and $E_{|2,1\rangle}$ [we define $E_{|2,1\rangle}$ with $V_1(z_{\min})$ added to it for plotting purposes], the cross mean-field energy, $E_{\mathrm{cross}} = N_2(2\pi\hbar^2 a_{12}/m)\langle\psi_1(t)||\psi_2|^2|\psi_1(t)\rangle$, and the total energy, $E_{\mathrm{tot}}(t_f) = E_{|2,2\rangle}(t_f) + E_{|2,1\rangle}(t_f) + E_{\mathrm{cross}}(t_f)$. $E_{|2,1\rangle}$ is large despite only 13% of the atoms being in this component because it is created with large potential energy. Figure 3 shows that the $|2,1\rangle$ and $|2,2\rangle$ wave packets collide around t_f

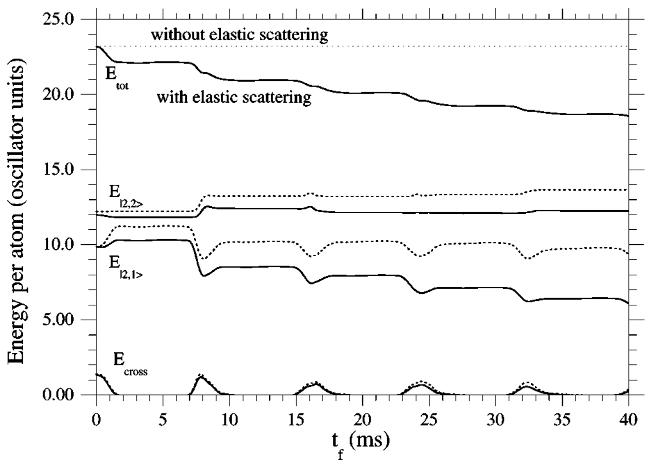

FIG. 3. Energies of the BEC wave packets versus time; solid lines are case (a) with full ESL, and dashed lines are case (b) without ESL. The total energy E_{tot} is the sum of the two component energies plus the energy associated with the overlap of the two components E_{cross}.

$=8,16,24,\ldots$ ms. This is evident from the increase in E_{cross} as the wave packets overlap, and in the exchange of energy between wave packets. The total energy per particle, E_{tot}, is constant in time unless ESL is included in the calculation. The effect of ESL is to remove atoms and a significant amount of energy from each of the wave packets. The fractional effect on the $|2,1\rangle$ wave packet is largest, since is has many fewer atoms to start with.

Figure 4 shows the calculated distribution of atoms in the two wave packets in the trap at times just before the first and fourth collisions of the wave packets near 8 and 32 ms, respectively. The figure shows the tendency of the smaller

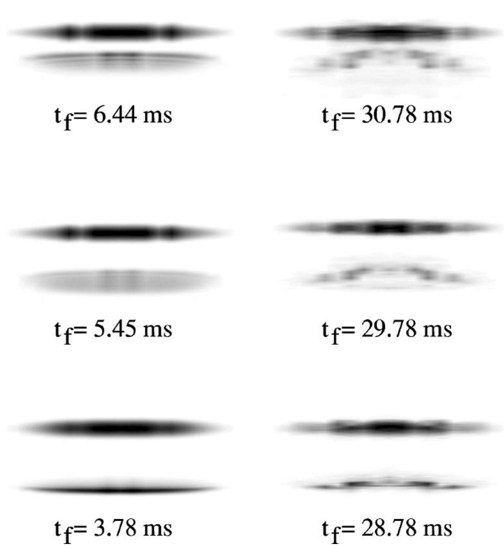

FIG. 4. $|2,1\rangle$ and $|2,2\rangle$ wave packets during the first and fourth oscillation cycles. In each of the six frames, the $|2,2\rangle$ wave packet is on the top. The frames on the left are for times before the first recollision of the $|2,1\rangle$ and $|2,2\rangle$ wave packets, and the frames on the right are before the fourth recollision. In each frame, the $|2,1\rangle$ wave packet is moving towards the $|2,2\rangle$ parent condensate.

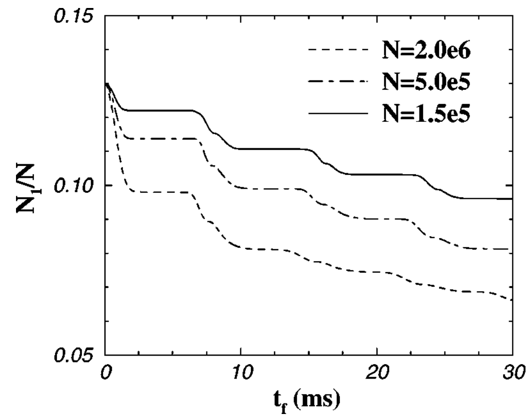

FIG. 5. Fraction of atoms in the $|2,1\rangle$ wave packet as a function of t_f. The number of atoms N in the initial parent $|2,2\rangle$ condensate is labeled in the legend. We assume full ESL (i.e., $\sigma=4\pi a_{12}^2$) in these examples.

$|2,1\rangle$ wave packet to break up and spread out after multiple collisions. Therefore, GPE calculations based on center-of-mass velocities may be less reliable after several wave-packet collisions. In addition, this breakup may make it more difficult to obtain an accurate experimental determination of the c.m. position of the $|2,1\rangle$ wave-packet trajectory at large t_f after multiple collisions. We expect that it will be most reliable to compare theory and experiment only after the first or second wave-packet collisions if possible.

B. New experiments to show ESL

The calculations described above indicate the importance of ESL and its suppression in BEC collision dynamics. It should be possible to detect ESL and its suppression in suitable BEC wave-packet collision experiments. Here we will examine ways that experiments of the type in Ref. [9] might be used to show such effects.

Unambiguously determining the extent of superfluid suppression of ESL might be obtained by simply expanding the clouds longer. This in principle would allow the variation in the velocity distributions of the different scattering models to be experimentally resolved. However, accurate measurements of the c.m. position will become more difficult as the cloud expands and becomes more dilute. Increasing the number of atoms in the parent condensate and therefore the $|2,1\rangle$ wave packet (while maintaining a 10–15 % ratio) would naturally allow the expansion time to be increased. Moreover, we find that increasing the number of atoms enhances the effects due to ESL.

Figure 5 shows the loss of atoms from the $|2,1\rangle$ wave packet (assuming full ESL) as a function of t_f for three different initial values of *N*. The two-million-atom case shows a 23% loss of atoms from the $|2,1\rangle$ wave packet in the initial half-collision. In this case, the effects of ESL are dramatic and immediately obvious in the first two oscillations of the $|2,1\rangle$ wave packet. We noted above why observing the collisional effects in the first couple of bounces is important due to $|2,1\rangle$ wave-packet breakup with increasing t_f. Figure 6 plots the calculated c.m. motion of the $|2,1\rangle$ and $|2,2\rangle$ condensates in the trap as a function of time duration t_f for *N*

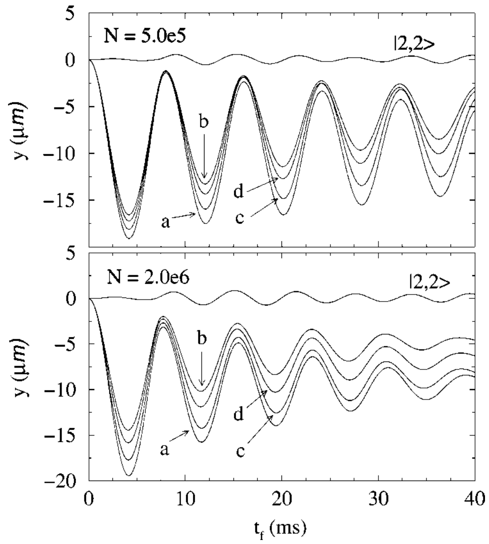

FIG. 6. Position of the center of mass of the $|2,1\rangle$ and the $|2,2\rangle$ wave packets in the magnetic trap versus t_f for $N=0.5\times10^6$ and 2.0×10^6 atoms. In each case, we assume 13% of the atoms are transferred into the initial $|2,1\rangle$ wave packet. Cases (a), (b), (c), and (d) are the same as described for Fig. 2.

$=0.5\times10^6$ and 2.0×10^6 atoms and $N_1=13\%\times N$. The four calculated curves shown in the figure correspond to cases (a), (b), (c), and (d) enumerated above. Now, there are clear differences between the c.m. motion that might be experimentally distinguishable. For the 2.0×10^6 case, large conversion of the $|2,1\rangle$ c.m. kinetic energy into the $|2,2\rangle$ kinetic energy occurs with a concomitant reduction in oscillation amplitude, even without ESL. Moreover, large differences in the amplitude of the remaining oscillatory motion is evident between the curves for the four different cases (a), (b), (c), and (d). If experimental imaging of the $|2,1\rangle$ wave packet inside the trap could be carried out, further information on ESL and its superfluid suppression could be obtained.

Figure 7 shows the calculated c.m. motion of the $|2,1\rangle$ wave packet 30 ms after the trap is turned off and the wave packet expands as it falls freely in gravity. For the case of 2.0×10^6 atoms, the difference between the c.m. motion with and without elastic scattering loss is about 33% in the first several bounces of the $|2,1\rangle$ wave packet. This should allow experimental verification of the effects of superfluid suppression, and perhaps even discrimination between more detailed models of superfluid suppression that may be developed in the future.

IV. SUMMARY

In summary, we have shown that the center-of-mass motion of colliding condensate wave packets composed of atoms having different internal states is sensitive to the ESL that can occur during the collision of the wave packets. Therefore, the types of experiments described here may be used to study ESL and superfluid suppression of ESL. From the detailed comparison with the data of Ref. [9], we conclude that ESL of atoms from the condensates is necessary in order to fit the data. However, it is difficult to determine the details of the superfluid suppression that occur. Future experiments with larger numbers of initial atoms as a function of trap frequencies and percentage of atoms converted to the $|2,1\rangle$ internal state will hopefully yield a detailed probe of superfluid suppression of ESL.

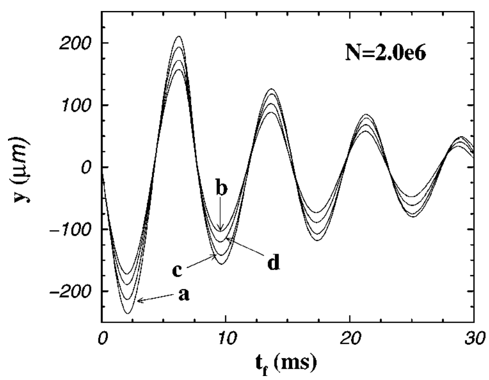

FIG. 7. Position of the center of mass of the $|2,1\rangle$ wave packet versus t_f for the $N=2.0\times10^6$ atom case after the wave packet has been allowed to fall under the influence of gravity for 30 ms. Cases (a), (b), (c), and (d) are the same as described for Fig. 2.

The bouncing condensate example we have treated is only meant to be illustrative of the type of effects that can occur in condensate collisions. It is clear from Refs. [1,4] and our present calculations that ESL will affect propagation of matter wave packets when they pass through each other, perhaps dramatically so. It is also clear from theoretical considerations and the measurements in Ref. [4] that suppression of ESL is expected when the relative collision velocities become sufficiently low. A variety of experiments that prepare and interact matter wave packets might be able to probe such effects. For example, experiments similar to that of Ref. [9] using a Raman pulse sequence rather than an rf pulse might allow greater control of the initial velocity of the condensate wave packets, thereby making it easier to determine the velocity dependence of superfluid suppression.

ACKNOWLEDGMENTS

We are grateful to the group of Professor Massimo Inguscio for valuable discussions. This work was supported in part by grants from the Office of Naval Research, the U.S.-Israel Binational Science Foundation, and the James Franck Binational German-Israeli Program in Laser-Matter Interaction.

[1] Y. B. Band, M. Trippenbach, J. P. Burke Jr., and P. S. Julienne, Phys. Rev. Lett. **84**, 5462 (2000).
[2] L. D. Landau, J. Phys. (Moscow) **5**, 71 (1941).
[3] K. Huang, *Statistical Mechanics* (John Wiley, New York, 1987).
[4] A. P. Chikkatur, A. Görlitz, D. M. Stamper-Kurn, S. Inouye, S. Gupta, and W. Ketterle, Phys. Rev. Lett. **85**, 483 (2000).
[5] P. O. Fedichev and G. V. Shlyapnikov, Phys. Rev. A **63**,

045601 (2001).
[6] E. Timmermans and R. Côté, Phys. Rev. Lett. **80**, 3419 (1998).
[7] M. Kozuma, L. Deng, E. W. Hagley, J. Wen, R. Lutwak, K. Helmerson, S. L. Rolston, and W. D. Phillips, Phys. Rev. Lett. **82**, 871 (1999).
[8] E. W. Hagley, L. Deng, M. Kozuma, J. Wen, K. Helmerson, S. L. Rolston, and W. D. Phillips, Science **283**, 1706 (1999).
[9] P. Maddaloni *et al.*, Phys. Rev. Lett. **85**, 2413 (2000).
[10] K. Bongs, *et al.*, Phys. Rev. Lett. **83**, 3577 (1999).
[11] B. Jackson, J. F. McCann, and C. S. Adam, Phys. Rev. A **61**, 051603 (2000).
[12] C. Raman *et al.*, Phys. Rev. Lett. **83**, 2502 (1999).
[13] K. Huang and C. N. Yang, Phys. Rev. **105**, 767 (1957).
[14] H. T. C. Stoof, M. Bijlsma, and M. Houbiers, J. Res. Natl. Inst. Stand. Technol. **101**, 443 (1996); N. P. Proukakis, K. Burnett, and H. T. C. Stoof, Phys. Rev. A **57**, 1230 (1998).
[15] P. Nozieres and D. Pines, *The Theory of Quantum Liquids* (Perseus Books, Cambridge, MA, 1999), Eq. (2.10).
[16] To obtain the correct phase of the CM motion, we had to turn off the magnetic field with a decay time $t_{\rm off}=0.5$ ms (private communication with the authors of Ref. [9]) as $B_i(t)=B_i(t_f)\exp[-(t-t_f)/t_{\rm off}]$. 3D simulations of short time expansions showed that the residual mean-field effects had little influence on the c.m. evolution.
[17] Numerical tests that included 50% additional atoms in a thermal cloud showed that the cloud is too dilute to significantly effect the amplitude or frequency shift of the $|2,1\rangle$ c.m. evolution.